

available at www.sciencedirect.comwww.elsevier.com/locate/brainres

**BRAIN
RESEARCH**

Research Report

Cross-frequency phase coupling of brain rhythms during the orienting response

Joseph R. Isler^{a,*}, Philip G. Grieve^{a,c}, D. Czernochowski^{b,d},
Raymond I. Stark^a, David Friedman^{b,d}

^aDepartment of Pediatrics, College of Physicians and Surgeons, Columbia University, P&S 3-440, 630 W. 168th Street, New York, NY 10032, USA

^bDepartment of Psychiatry, Columbia University, USA

^cDepartment of Biomedical Engineering, Columbia University, USA

^dCognitive Electrophysiology Laboratory, New York State Psychiatric Institute, USA

ARTICLE INFO
Article history:

Accepted 2 July 2008

Available online 16 July 2008

Keywords:

Bicoherence

Cross-frequency coupling

Orienting response

Novelty

P3

Coherence

ABSTRACT

A critical function of the brain's orienting response is to evaluate novel environmental events in order to prepare for potential behavioral action. Here, measures of synchronization (power, coherence) and nonlinear cross-frequency phase coupling ($m:n$ phase locking measured with bicoherence and cross-bicoherence) were computed on 62-channel electroencephalographic (EEG) data during a paradigm in which unexpected, highly-deviant, novel sounds were randomly intermixed with frequent standard and infrequent target tones. Low frequency resolution analyses showed no significant changes in phase coupling for any stimulus type, though significant changes in power and synchrony did occur. High frequency resolution analyses, on the other hand, showed significant differences in phase coupling, but only for novel sounds compared to standard tones. Novel sounds elicited increased power and coherence in the delta band together with $m:n$ phase locking (bicoherence) of delta:theta (1:3) and delta:alpha (1:4) rhythms in widespread fronto-central, right parietal, temporal, and occipital regions. Cross-bicoherence revealed that globally synchronized delta oscillations were phase coupled to theta oscillations in central regions and to alpha oscillations in right parietal and posterior regions. These results suggest that globally synchronized low frequency oscillations with phase coupling to more localized higher frequency oscillations provide a neural mechanism for the orienting response.

© 2008 Elsevier B.V. All rights reserved.

1. Introduction

The orienting response is a fundamental biological mechanism that is necessary for survival (Luria, 1973). It is a rapid response to new, unexpected or unpredictable events that entails the involuntary (so-called “bottom up”) capture of

attention and essentially functions as a “what-is-it” detector (Sokolov, 1990). The neural correlates of the orienting response in humans have been most often studied by recording event-related potentials (ERPs) during the auditory novelty oddball paradigm. In that paradigm, stimuli consist of a frequent tone (the standard) randomly interspersed with

* Corresponding author. Fax: +1 212 305 0956.

E-mail address: jri2101@columbia.edu (J.R. Isler).

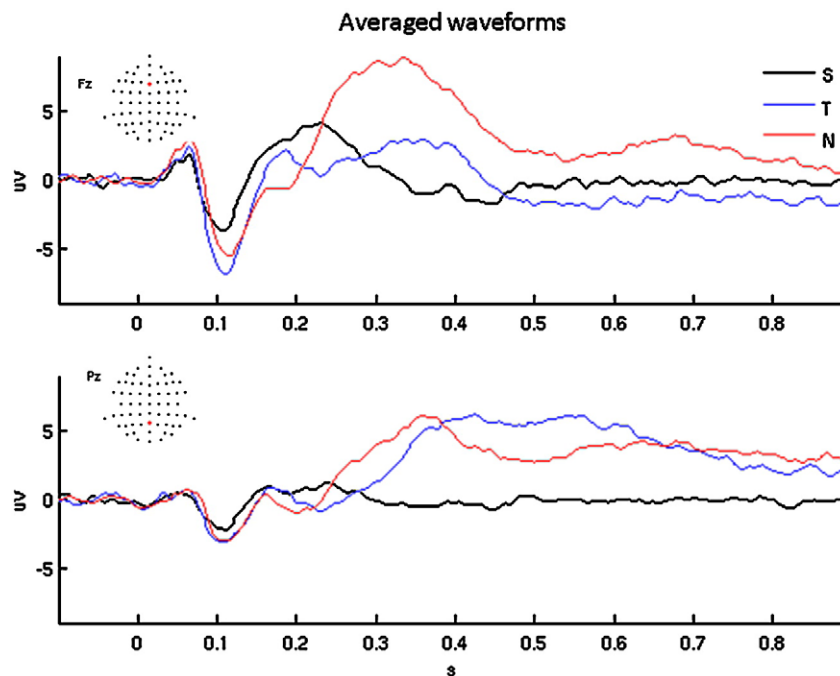


Fig. 1 – Averaged waveforms. Grand average waveforms for standard tones (S, black), target tones (T, blue), and novel, environmental sounds (N, red). Top: frontal electrode (Fz); bottom: posterior electrode (Pz).

less frequent target tones and novel sounds. The latter are a set of unexpected environmental sounds that occur only once per experiment. A great deal of research has indicated that the P3 component of the ERP elicited by novel sounds is an electrophysiological correlate of the orienting response (Friedman et al., 2001). This novelty P3 (called P3a) is distinct from the P3 elicited by equally-infrequent target tones (called P3b) in its cognitive correlates, surface topography and intracranial sources. Widespread posterior, parietal, and temporal areas contribute to the P3b and widespread frontal, parietal, and temporal areas contribute to the P3a (Friedman et al., 2001; Ranganath and Rainer, 2003). These electrophysiological studies of the orienting response have primarily been carried out in the time domain by analyzing amplitudes, latencies, and intracranial source models of ERP components. Complementary analysis of EEG recordings in the frequency domain makes it possible to directly quantify known neural mechanisms such as synchronization and cross-frequency coupling of field potential oscillations (Isler et al., 2007). Such analyses provide a framework to investigate how the distributed neuronal networks that underpin the orienting response act in concert to determine what the deviant, environmental perturbation represents, evaluate its significance, and prepare for a possible behavioral response.

Synchronization of oscillations in electric field potentials within and between brain regions is an efficient mechanism for coalescing local and regional assemblies into more widespread networks (Varela et al., 2001). Oscillatory synchrony can function as a fundamental mechanism in both perception (Gray et al., 1989; Tallon-Baudry et al., 1996) and behavior control (Pfurtscheller et al., 1994; von Stein et al.,

2000). Membrane potential oscillations precipitate plasticity (LTP/LTD) even in the absence of post-synaptic action potentials, i.e. without Hebbian plasticity (Golding et al., 2002). Furthermore, at least for some brain rhythms and regions, information is encoded in the phase of oscillatory activity (O’Keefe and Recce, 1993). Phase encoding offers a rich modality for “putting oscillations to work” in the brain and has been proposed as a potential mechanism for working memory (Buzsaki, 2005; Jensen and Lisman, 1998). We hypothesized that it could be a brain mechanism for the orienting response.

Increasingly, there is evidence that oscillations in the traditional EEG frequency bands (delta 1–4 Hz, theta 4–8 Hz, alpha 8–12 Hz, beta 12–25 Hz, gamma > 25 Hz) are manifestations of, and may even facilitate, different cognitive functions (Buschman and Miller, 2007; Buzsaki and Draguhn, 2004), although the mapping from function to frequency may not be unique and may be dynamically and spatially variable (Palva and Palva, 2007). For example, the theta band is associated with memory and information transfers between neocortex and hippocampus (Kahana et al., 2001) while the gamma band is associated with stimulus feature binding, localized representations, and awareness (Bertrand and Tallon-Baudry, 2000; Lachaux et al., 2000; Rodriguez et al., 1999). Consequently, coupling of oscillatory activity across frequency bands (cross-frequency coupling) provides a simple mechanism whereby distinct cognitive functions can operate conjointly to perform a given task (Jensen and Colgin, 2007). Cross-frequency coupling in which the amplitude of one frequency is modulated by the phase of another frequency (phase-amplitude coupling) has been observed in intracortical recordings (Canolty et al., 2006) in

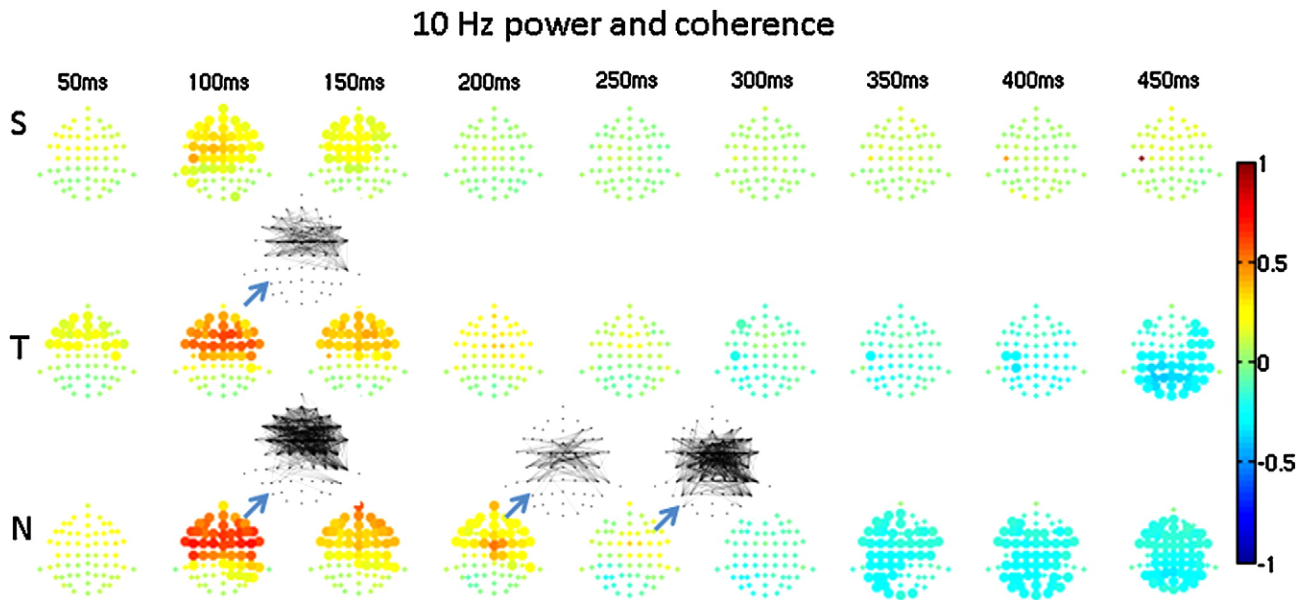


Fig. 2 – 5 to 15 Hz power and coherence. Low frequency resolution analysis at a center frequency of 10 Hz. Fractional change from pre-stimulus power in overlapping 100 ms windows is shown by balls at the scalp electrode locations with fractional values shown in color. Large ball sizes denote significant changes. At the blue arrows, significant changes from baseline coherence are shown by lines connecting electrode locations, with increases in coherence shown by black lines (no significant decreases in coherence occurred). In determining significance, p -values were corrected for multiple comparisons with a false discovery rate of 0.05. Note: power in the 0 to 5 Hz band was similar to that shown here, but coherence could not be measured in that band.

both spontaneous and task-related activity and has led to the idea of an oscillatory hierarchy made up of nested phase-amplitude relationships (Lakatos et al., 2005). Another form of cross-frequency coupling is phase-phase coupling (or $m:n$ phase locking, or simply phase coupling) which occurs as the result of nonlinear interactions between frequencies, though it can also arise due to nonlinear distortions, autoresonance, and other nonlinear processes. Demonstration of this form of coupling has been made *in vitro* (Gloveli et al., 2005) and *in vivo* (Palva et al., 2005; Schack et al., 2002). With phase coupling, information encoded in the phase of the higher frequency is preserved across multiple cycles of the lower frequency rhythm. This provides a mechanism for multiplexing the activity in a single neuron or local neuronal population because the same neuron(s) can simultaneously phase-encode at multiple frequencies.

The goal of the present study was to determine if cross-frequency phase coupling of electric potential oscillations occurs as part of the brain's orienting response to unexpected environmental stimuli. We hypothesized that it would, under the assumption that neuronal networks exhibiting synchronized oscillations at different frequencies (perhaps subserving distinct cognitive functions) would be interacting during the orienting response. We tested our hypothesis by quantifying synchronization and cross-frequency phase coupling of brain oscillations in the auditory novelty oddball paradigm. Specifically, we hypothesized that cross-frequency phase coupling would be greater for novel sounds than for target and standard tones. Furthermore, we expected regional synchronization to be greater for target than standard tones, and even greater for

novel sounds than targets, with a spatial distribution that was more anterior for novels and more posterior for targets.

2. Results

Fig. 1 shows grand-averaged waveforms for frontal (Fz, top) and posterior electrodes (Pz, bottom) for the three stimulus types. As in previous studies, all three stimuli elicit a P1–N1–P2 complex at early latencies (<200 ms) while novel sounds elicit a large positive potential over frontal regions at approximately 300 ms post-stimulus whereas target tones elicit a somewhat later and broader positive potential over posterior regions (Friedman et al., 2001). Frequency-domain measures of synchrony and coupling were then the focus of subsequent analyses to further differentiate these three types of stimuli.

2.1. Low frequency resolution analysis (10 Hz frequency resolution, 100 ms intervals, 50 ms overlap)

Significant differences were determined as change from a pre-stimulus 100 ms interval. In the lowest frequency bin (0–5 Hz, not shown) power results were similar to those shown for the 10 Hz band. In the 10 Hz band (5–15 Hz, Fig. 2), significant increases in power occurred over frontal regions for all three stimulus types at 100 and 150 ms (i.e. 50–200 ms). The magnitude of the increase was greatest for the novel (~100%), smaller for the target (~50%) and lowest for the standard (~25%). Only the novel had a significant power

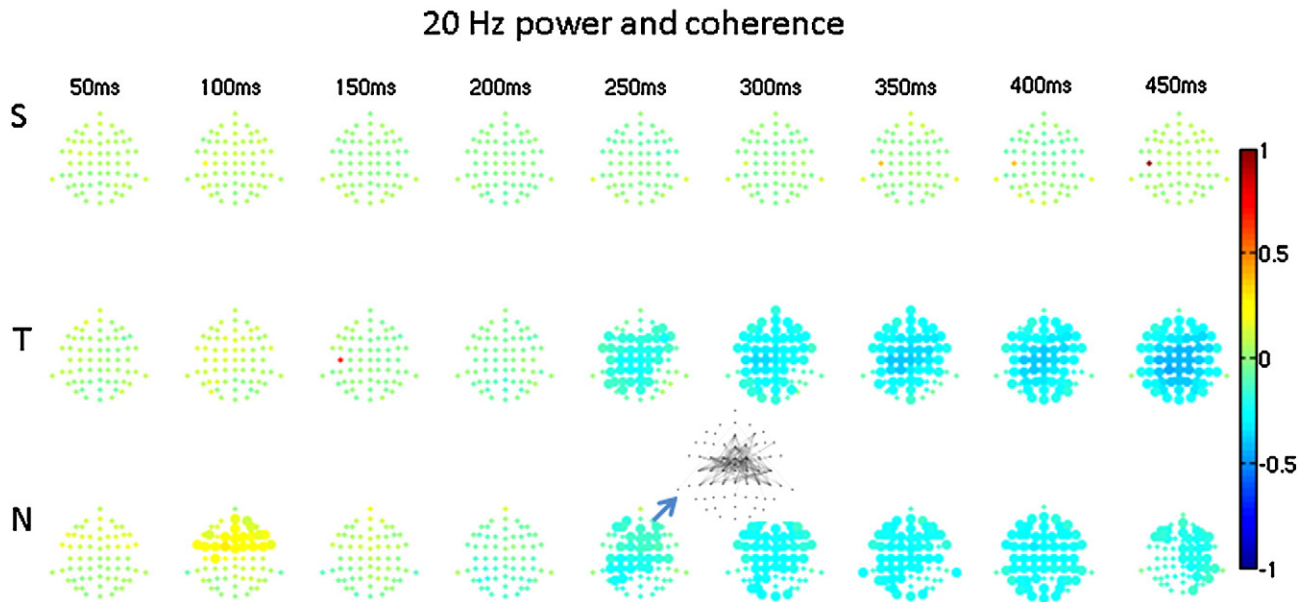


Fig. 3 – 15 to 25 Hz power and coherence. As in Fig. 2, but at a center frequency of 20 Hz. The only significant change in coherence occurred for novel sounds as increased coherence over widespread frontal areas at 200–300 ms post-stimulus. Note that during the same interval there was a concomitant decrease in band power.

increase at 200 ms (i.e. 150–250 ms). Significant power decreases (“desynchronization”, (Pfurtscheller and Andrew, 1999)) of 20 to 40% occurred at later latencies (>250–300 ms) for both the novel and target but not for the standard. This decrease continued beyond 500 ms (not shown). There were no significant changes in coherence for the standard but there were widespread increases in coherence over frontal and central regions for the target at 150 ms and for the novel at 150, 200, and 250 ms. Interestingly, the widespread increase in coherence for the novel at 250 ms occurred when there was no (significant) concomitant increase in power, and furthermore all increases in coherence for the novel and target occurred before 300 ms.

In the 20 Hz band (15–25 Hz, Fig. 3) the only significant increase in coherence occurred for the novel at 250 ms when there was a concomitant significant 10 to 20% decrease in power. In higher frequency bands there were no significant changes in coherence and there were no power increases, though there continued to be decreased power for the target and novel stimuli at later latencies (>250 ms). Bicoherence and cross-bicoherence showed no significant changes for any frequency pairs.

To summarize, low frequency resolution analyses revealed widespread synchronization over frontal areas that was greatest for novel sounds and least for standard tones at early (<200 ms) latencies while at later times (>200 ms) widespread frontal synchronization occurred only for novel sounds. There was no evidence of cross-frequency phase coupling.

2.2. High frequency resolution analysis (2.2 Hz frequency resolution, 448 ms intervals, 224 ms overlap)

Significant differences were determined by comparisons between stimulus types. At the lowest frequency of approxi-

mately 2.2 Hz (Fig. 4), novel and target power were higher than that of the standard. The largest differences (~500%) occurred for novel vs. standard at 224 ms (i.e. 0–448 ms). Generally, less pronounced differences were found with increasing post-stimulus time. Novel power was greater than target power over frontal regions at 224 ms while it was less than target power over posterior regions at 448 ms (i.e. 326–570 ms). Coherence was significantly greater for target than standard across predominantly posterior regions over the entire post-stimulus interval. At 224 ms, coherence was greater for the novel than standard across the entire scalp, while coherence was greater for the novel than target over most of the scalp except occipital regions.

At 4.5 Hz (Fig. 5), power differences were similar to those at 2.2 Hz except there were fewer significant differences at longer latencies. Target vs. standard coherence differences were similar to those at 2.2 Hz, whereas the novel produced significantly greater coherence than the standard for all post-stimulus intervals. These included widespread posterior coherence at 448 ms when concomitant power differences were modest. There was no significant coherence difference between novel and target. At 6.7 Hz (not shown) novel and target power were greater than that of the standard over fronto-central regions at 224 ms; there were no significant coherence differences. At 9.0 Hz (not shown) there was a modest target-standard contrast at 224 ms over orbito-frontal regions and a widespread novel-standard difference (standard>novel) at 448 ms over frontal regions; there were no significant coherence contrasts. In higher frequency bands, power and coherence contrasts failed to meet the false discovery rate criterion of 0.05.

Bicoherence and cross-bicoherence were significantly different between stimulus types only at 224 ms (0–448 ms) for novel-standard (but not for target-standard or novel-

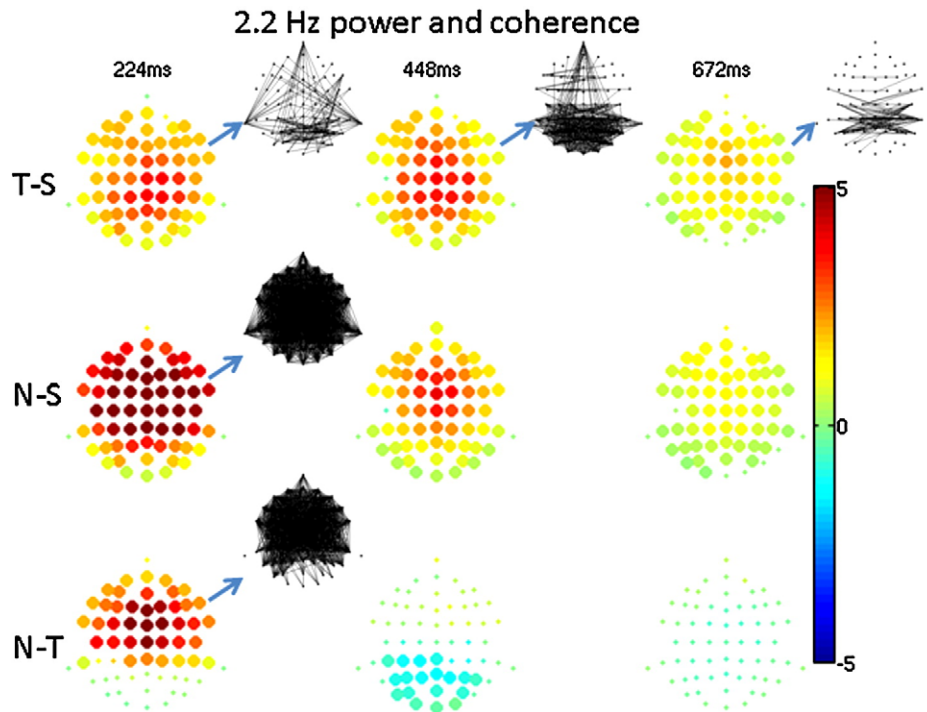


Fig. 4 – 2.2 Hz power and coherence. High frequency resolution (2.2 Hz bandwidth) analysis at the lowest frequency of 2.2 Hz. The fractional difference in power between conditions in overlapping 448 ms windows is shown by balls at the scalp electrode locations with fractional values shown in color. Large ball sizes denote significant differences. At the blue arrows, significant differences in coherence are shown by lines connecting electrode locations, with positive differences shown by black lines (no significant negative differences occurred). Differences were taken as target minus standard (denoted T–S), novel minus standard (N–S), and novel minus target (N–T). In determining significance, *p*-values were corrected for multiple comparisons with a false discovery rate of 0.05.

target) in two frequency couplings: 1:3 phase locking (2.2 Hz to 6.7 Hz, Fig. 6, and 1:4 phase locking (2.2 Hz to 9.0 Hz, Fig. 7). In both cases, bicoherence (Figs. 6A and 7A, respectively) was widespread over the head but showed the largest coupling effects (~ 0.1) over central and parietal regions with a rightward bias. The region showing the largest 1:4 phase locking (delta:alpha) was slightly more posterior than the region showing the largest 1:3 phase locking (delta:theta). Matrices of cross-bicoherence for the corresponding cases (Figs. 6B and 7B) have a sparse columnar structure, showing that the higher frequency (6.7 Hz or 9.0 Hz) within a localized region (central-parietal or posterior-right-central-parietal, respectively) was phase coupled to the lower frequency (2.2 Hz) over the entire head (insets in Figs. 6B and 7B). Note that 4.5 Hz showed significant within-frequency synchronization (power and coherence) differences between conditions (Fig. 5) yet this frequency did not couple to other frequencies, illustrating that synchrony and nonlinear coupling are distinct mechanisms.

To summarize, high frequency resolution analyses revealed widespread synchronization contrasts across all three conditions, primarily in the delta and theta bands, with the greatest differences for the novel-standard comparison. Further, for the novel-standard comparison, there was evidence of widespread cross-frequency phase coupling of delta:theta and delta:alpha rhythms, with globally distributed delta oscillations phase

coupled to more localized theta and alpha oscillations in central and right parietal/posterior regions, respectively.

3. Discussion

We hypothesized that cross-frequency phase coupling of electric field potential oscillations would occur for novel environmental sounds but not for target and standard tones in an auditory novelty oddball experiment. In support of our hypothesis, there was widespread coupling of delta:theta and delta:alpha rhythms for novel sounds compared to standard tones, but no significant coupling was observed for targets compared to standards. The lack of coupling in the latter case suggests that cross-frequency phase coupling is a neural mechanism underlying the orienting response because target tones, unlike novel environmental sounds, do not elicit the orienting response (reflected in its neural correlate, the frontally-biased P3a).

As noted in the Introduction, there is recent evidence that different frequency bands of field potential oscillations correlate with different cognitive functions, albeit with the caveat that the mapping from function to frequency may not be unique and may be dynamically and spatially variable. The findings presented here are in accord with this emerging view

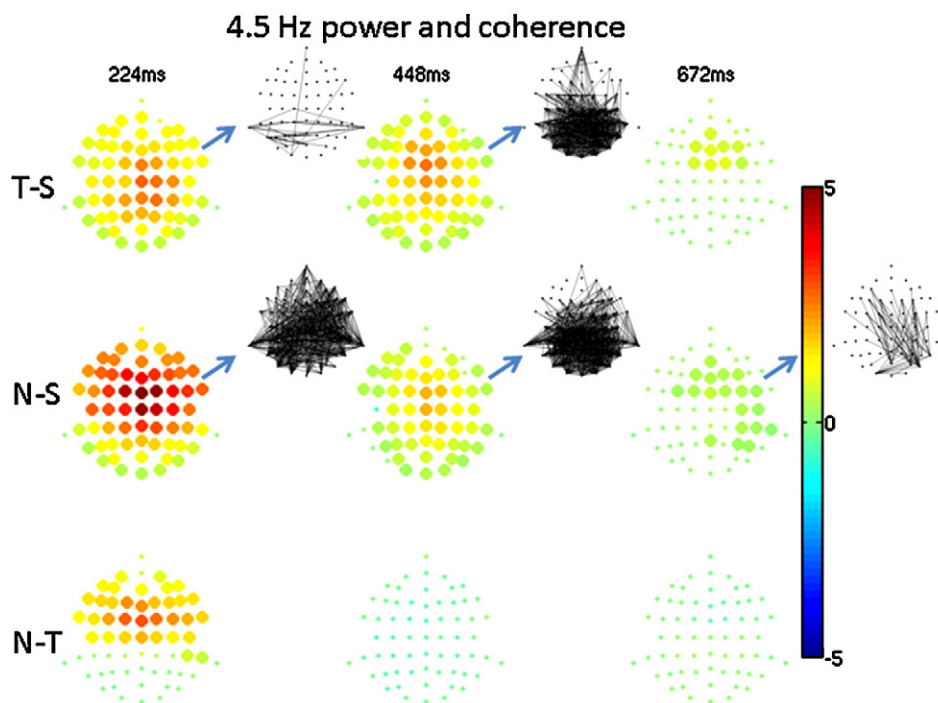


Fig. 5 – 4.5 Hz power and coherence. As in Fig. 4, but at 4.5 Hz.

of functionally distinct roles for oscillations in electric field potential. When a novel sound is heard, arousal and attention are heightened and memory and sensory networks are engaged to determine identity. The phase coupling between field potential oscillations observed in this study could provide a mechanism for the coordination of these activities across specialized networks.

Complementary analysis windows were used for high temporal or frequency resolution, suitable for the FFT-based methods used here. At high temporal resolution, frequency resolution was too poor (10 Hz) to capture significant changes in phase coupling between frequencies (bicoherence and cross-bicoherence). This is perhaps not surprising, since putatively distinct network oscillations (e.g. theta and alpha) would be merged into one frequency band. Similarly, delta band phase could not be resolved (occurring in the DC frequency bin) so phase coupling between delta and other frequencies could not be measured. In contrast, changes in synchronization (power and coherence) were significant at high temporal resolution. In support of our expectation and previous ERP studies, synchronization increases were greatest for novel sounds, lesser for targets, and lesser still for standard tones. Interestingly, power and coherence at 10 and 20 Hz distinguished the three stimulus types at early latencies (50–150 ms), much earlier than the prominent P3a and P3b components at approximately 300 ms. Indeed, targets and novels produced *decreased* power at longer latencies. What distinguished novel sounds from both target and standard tones at approximately 300 ms was widespread 10 and 20 Hz coherence across frontal regions. These results demonstrate the value of frequency-domain analysis compared to traditional time-domain (ERP) analysis, as mentioned in the Introduction, viz., frequency-domain measures directly quan-

tify known neural mechanisms such as synchronization and cross-frequency coupling of field potential oscillations (Isler et al., 2007).

At high frequency resolution, temporal resolution is too low (448 ms) to allow for a comparison with a pre-stimulus interval in these data. However, comparisons could be made between stimulus types with sufficient frequency resolution to measure phase in the delta band and dissociate theta and alpha rhythms. As expected, novels elicited a more frontal pattern of synchronization than targets (N–T in Figs. 4 and 5). Furthermore, in support of our phase coupling hypothesis, bicoherence and cross-bicoherence analyses revealed significantly greater delta:theta and delta:alpha phase coupling for novel sounds compared to standard tones. Phase coupling (bicoherence) contrasts were widespread with largest magnitudes over central and right parietal areas for delta:theta coupling (Fig. 6A) but over right central, parietal and posterior areas for delta:alpha coupling (Fig. 7A). Cross-regional phase coupling (cross-bicoherence) contrasts revealed a global (i.e. over the entire scalp) delta oscillation coupling to theta (Fig. 6B) and alpha (Fig. 7B) oscillations localized to central and right parietal/posterior regions, respectively. This coupling suggests a mechanism whereby a cognitive property of the global network (e.g., arousal) affects processing in more localized and specialized networks, though it is impossible in the present study to associate specific cognitive correlates to the observed delta:theta and delta:alpha coupling. Interestingly, the narrow 4.5 Hz band (high delta/low theta) does not participate in any significant phase coupling with other bands despite its robust synchronization response in power and coherence. These findings support the view that the distinct frequency bands serving cognitive functions can be quite narrow (Buzsaki and Draguhn, 2004). This is of

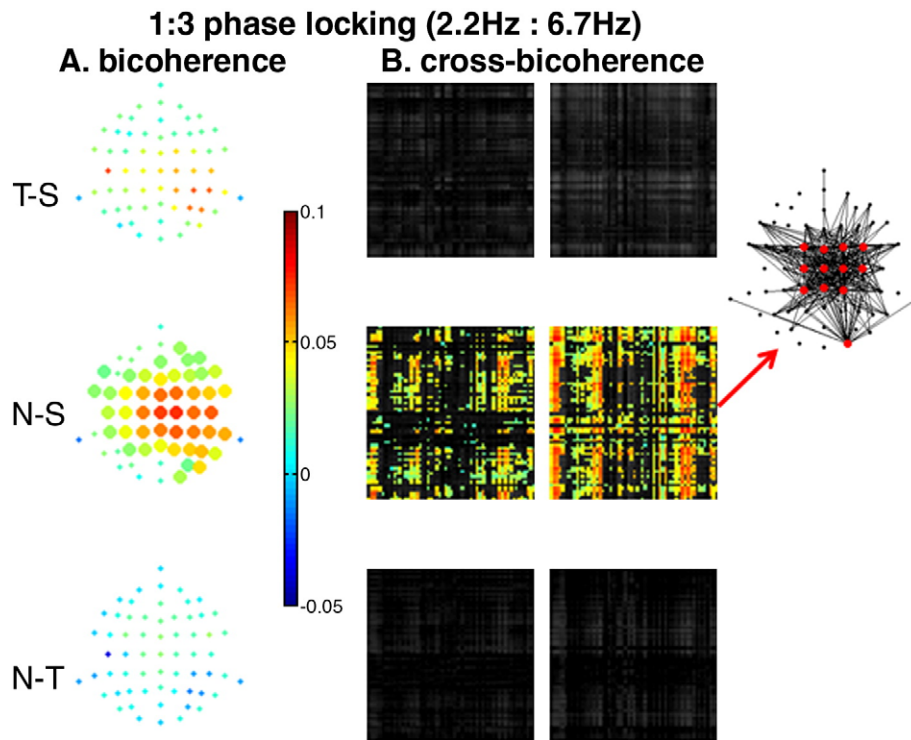


Fig. 6 – 1:3 phase locking. Delta:theta bicoherence (A) and cross-bicoherence (B) differences at 0–450 ms. (A) Difference in 1:3 phase locking (bicoherence between 2.2 and ~6.7 Hz) is shown by balls at all electrode locations, with difference values shown in color. Large ball sizes denote significant differences. As in Figs. 4 and 5, T–S denotes target minus standard, N–S denotes novel minus standard, and N–T denotes novel minus target. In determining significance, p -values were corrected for multiple comparisons with a false discovery rate of 0.05. (B) Difference in cross-electrode 1:3 phase locking (cross-bicoherence between 2.2 and ~6.7 Hz) is shown for all electrode pairs by 62×62 (electrode by electrode) matrices, with 2.2 Hz in the row electrode, 6.7 Hz in the column electrode, and the sum frequency in the row electrode (left) or column electrode (right). Significant differences are shown in color with the same color scale as in A. In determining significance, p -values were corrected for multiple comparisons with a false discovery rate of 0.05. The columnar structure of the cross-bicoherence matrices shows that theta (6.7 Hz) oscillations at a discrete set of locations (predominantly central and parietal regions) couple to a global delta (2.2 Hz) oscillation. At the red arrows, the topography of cross-bicoherence is illustrated by lines connecting electrode locations for pairs involving the 12 electrodes (red) with the highest pairwise mean differences.

importance because a narrow band would allow for more precise and reliable phase encoding.

Taken together, the two time-frequency analyses complement each other. High temporal resolution analysis revealed widespread but transient synchronization that persisted longest in response to novelty, while low temporal resolution analysis revealed phase coupling of brain rhythms that was narrow-band frequency specific and topographically differentiated. However, it should be noted that care must be taken when comparing results across the two time-frequency analyses. For example, there are only modest alpha power contrasts in the high frequency resolution (448 ms window) analysis while there are large changes in alpha power and coherence in the low frequency resolution (100 ms window) analysis. The 448 ms analysis assesses differences between stimulus types and is most sensitive to narrow-band activity that persists for several hundred milliseconds. The 100 ms analysis measures a change from pre-stimulus levels for a given stimulus type and is better able to detect broad band

transient (less than ~100 ms) activity. Indeed, it can be seen in the latter case (Fig. 2) that alpha power and coherence vary considerably across the first 500 ms, with initial power increases for novels and targets followed by decreased power. This variability could account for the lack of significant contrast in alpha power between stimulus types across a 448 ms window. It should also be noted that the lack of significant synchrony and coupling involving gamma band frequencies may have more to do with the difficulty of observing that band in adult scalp data than in the absence of such synchrony and coupling per se. Finally, bivariate measures (coherence and cross-bicoherence) can be biased by volume conduction when nearby electrodes have overlapping source regions. As mentioned in the Experimental procedures section below, evaluation of differences removes baseline bias. However, if power (or bicoherence) changes from its baseline level (or between conditions), that change will confound changes in coherence (or cross-bicoherence) because the area of overlapping source regions will increase.

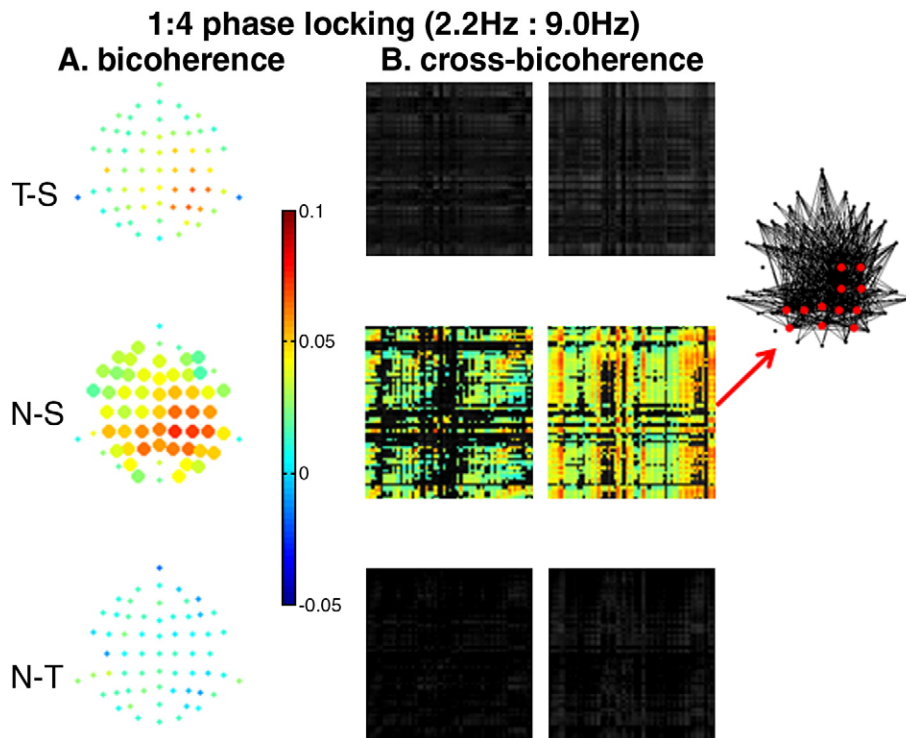


Fig. 7 – 1:4 phase locking. Delta:alpha bicoherence (A) and cross-bicoherence (B) differences at 0–450 ms. As in Fig. 6, but for 1:4 phase locking (bicoherence and cross-bicoherence between 2.2 and 9.0 Hz). In B, 9.0 Hz is in the column electrode and 2.2 Hz is in the row electrode. Note in A that the distribution of bicoherence differences is more posterior than in Fig. 6A, while in B localized alpha (9.0 Hz) oscillations, predominantly in posterior and right central and parietal regions, couple to a global delta (2.2 Hz) oscillation.

However, the coherence and cross-bicoherence results presented here include many pairs of distant electrodes, making volume conduction an unlikely explanation of the effect for these numerous distant pairs.

In summary, the results presented here suggest that cross-frequency phase coupling, specifically delta oscillations synchronized globally and phase coupled to more localized higher frequency oscillations, is a neural mechanism underlying the brain's orienting response. This mechanism links globally distributed but localized theta and alpha oscillations without the necessity for global synchrony in those bands. Through phase coupling, information encoded locally in the phase of the higher frequency oscillation is preserved across cycles of the global delta oscillation, providing a mechanism for multiplexing the phase encoding of single neurons or clusters of functional neuronal columns. We speculate that this mechanism could be the substrate for the cooperative interaction of the multiple networks engaged in processing and identifying novelty.

4. Experimental procedures

4.1. Subjects

The subjects were 13 normal right-handed older adults (5 male) aged 54 to 83 (mean 72) who provided informed consent in accord with the Institutional Review Board at the New York

State Psychiatric Institute. This was a secondary analysis of a dataset studying aging. We used this dataset because it offered sufficient power to test our hypotheses and not as a study of aging per se.

4.2. Protocol, recording, pre-processing

Subjects were seated in a sound-damped, electrically-shielded room. Sound trains were presented in 10 blocks (80 trials per block) and consisted of frequent, standard ($p=0.8$) infrequent, target tones ($p=0.1$) and 48 novel, environmental sounds ($p=0.1$). The tones were 700 and 1000 Hz (counterbalanced between target and standard across subjects). Sounds were presented via headphones at approximately 80 dB sound pressure level at the subject's ears. The inter-stimulus-interval was 1 s. Subjects were instructed to press a response button (emphasizing speed) only to the target tone. EEG was recorded with sintered Ag/AgCl electrodes mounted in an elastic cap (Neuromedical Supplies) from 62 scalp sites in accordance with the extended 10–20 system. Vertical electrooculogram (EOG) was recorded from electrodes placed above and below the left eye and horizontal EOG from electrodes placed at the outer canthus of each eye. Electrode impedance was kept below 5 k Ω . The activity at all scalp electrodes was recorded referenced to the nosetip and re-referenced offline to averaged mastoids. EEG and EOG were recorded continuously with Synamp amplifiers (0–100 Hz; 500 Hz digitization). Trials were

segmented into 100 ms pre- and 900 ms post-stimulus intervals. Muscular and other artifact were rejected by visual inspection on a trial by trial basis. If single channels showed artifacts, up to 3 channels on a given trial were rebuilt by spherical spline interpolation (Perrin et al., 1987). Blinks and horizontal eye movements were corrected (Gratton et al., 1983).

4.3. Data analysis

Because of time–frequency tradeoffs, frequency-domain analyses were performed twice. Low frequency resolution analysis used overlapping 100 ms intervals and comparisons were made to the pre-stimulus interval. High frequency resolution analysis used three 448 ms intervals (with 50% overlap) and comparisons were made between stimulus types (i.e. standards, targets, novels). The number of standard trials used in both analyses was reduced to be approximately the same as the other stimuli (by taking the first 1/8) to avoid confounding statistical effects in comparisons between stimulus types. Averaged waveforms were computed as the mean voltage across trials at each electrode with the removal of the mean voltage over the 100 ms pre-stimulus interval.

Synchronization of oscillations within a frequency band was quantified by power and coherence. Transmembrane currents due to EPSP/IPSP activity produce the electric field recorded on the scalp (Nunez, 1981); thus power at a single electrode quantifies the degree of synchronized input in the underlying cortical region. Coherence between pairs of electrodes was used to quantify the degree of synchrony between the corresponding regions, albeit biased by volume conduction effects dependent on inter-electrode distance (Srinivasan et al., 1998). This baseline bias is removed when coherence differences are taken, as in this study, though changes from baseline power confound coherence differences except for distant pairs of electrodes. Fast Fourier transforms (FFTs) were taken for each interval after de-meaning and application of a Hanning window (Bendat and Piersol, 2000). Power spectra were the magnitude-squared FFTs averaged across trials (the numerator of Eq. (1) (below) with $i=j$). Cross spectra were calculated by averaging the product of one channel FFT with the complex conjugate FFT of another channel for all possible pairs (i,j) of channels across trials; coherence, $C_{ij}(f)$, was defined as the magnitude of the cross spectrum normalized by the square root of the product of the channel powers (Bendat and Piersol, 2000), viz.

$$C_{ij}(f) = \langle X_i(f)X_j^*(f) \rangle / \left[\langle |X_i(f)|^2 \rangle \langle |X_j(f)|^2 \rangle \right]^{1/2} \quad (1)$$

where $X_i(f)$ and $X_j(f)$ are the frequency(f)-dependent complex Fourier transforms of the two time(t) series $x_i(t)$ and $x_j(t)$ and the brackets represent an expectation value.

Coupling of oscillations across frequency bands was quantified by bicoherence and cross-bicoherence. Bicoherence measures the degree of quadratic phase coupling between frequencies in a single time series; cross-bicoherence measures quadratic phase coupling between frequencies across two times series. Quadratic phase coupling occurs as a result of nonlinear (second-order) interactions between oscillators which give rise to sum frequencies. It is expressed as

$$2\pi f_3 t + \phi_3 = 2\pi f_1 t + \phi_1 + 2\pi f_2 t + \phi_2 \quad (2)$$

which requires both $f_3=f_1+f_2$ and $\phi_3=\phi_1+\phi_2$; in other words not only is a sum frequency present but its phase (ϕ) is not randomly distributed with respect to the other phases. Bicoherence was calculated using the product of the FFT at two different frequencies times the complex conjugate of the FFT at the sum of the two frequencies, normalized by the product of FFTs at the three frequencies (Eq. (3) below, with $i=j$) (Nikias and Petropulu, 1993). Cross-bicoherence, $B_{ij}(f_1,f_2)$, between electrode pairs (i,j) was calculated using the product of the FFT at two different frequencies (f_1,f_2) and electrodes multiplied by the complex conjugate of the FFT at the sum of the two frequencies at one of the electrodes, normalized by the product of FFTs at the three frequencies, viz.

$$B_{ij}(f_1,f_2) = \langle X_i(f_1)X_j(f_2)X_j^*(f_1+f_2) \rangle / \left[\langle |X_i(f_1)|^2 \rangle \langle |X_j(f_2)|^2 \rangle \langle |X_j(f_1+f_2)|^2 \rangle \right]^{1/2} \quad (3)$$

The cross-bicoherence for a pair of frequencies is thus represented by two electrode by electrode matrices: one where the sum frequency is detected in the row electrode and one where it is in the column electrode.

Subsequently, change scores were either the difference taken against a baseline interval in the low frequency resolution analysis or the difference between conditions in the high frequency resolution analysis. Fractional differences were used for power. Group statistics (mean, standard error) were calculated for all change scores and t-tests were used to determine significance for each electrode (for power and bicoherence) or pair of electrodes (for coherence and cross-bicoherence). To correct for multiple comparisons across electrodes (or across all electrode pairs for coherence and cross-bicoherence), a false discovery rate of 0.05 was used (Genovese et al., 2002). It is important to note that all phase-dependent measures (i.e. coherence, bicoherence, and cross-bicoherence, but not power spectra) are ill-defined for the lowest (DC) frequency and so results are not presented at those frequencies.

Acknowledgments

National Institutes of Health (NINDS 5K25NS052230 to J.I., NIA AG005213 to D.F.).

REFERENCES

- Bendat, J.S., Piersol, A.G., 2000. Random Data: Analysis and Measurement Procedures, Vol. Wiley, New York.
- Bertrand, O., Tallon-Baudry, C., 2000. Oscillatory gamma activity in humans: a possible role for object representation. *Int. J. Psychophysiol.* 38, 211–223.
- Buzsaki, G., Draguhn, A., 2004. Neuronal oscillations in cortical networks. *Science* 304, 1926–1929.
- Canolty, R.T., Edwards, E., Dalal, S.S., Soltani, M., Nagarajan, S.S., Kirsch, H.E., Berger, M.S., Barbaro, N.M., Knight, R.T., 2006. High gamma power is phase-locked to theta oscillations in human neocortex. *Science* 313, 1626–1628.

- Friedman, D., Cycowicz, Y.M., Gaeta, H., 2001. The novelty P3: an event-related brain potential (ERP) sign of the brain's evaluation of novelty. *Neurosci. Biobehav. Rev.* 25, 355–373.
- Genovese, C.R., Lazar, N.A., Nichols, T., 2002. Thresholding of statistical maps in functional neuroimaging using the false discovery rate. *NeuroImage* 15, 870–878.
- Gloveli, T., Dugladze, T., Rotstein, H.G., Traub, R.D., Monyer, H., Heinemann, U., Whittington, M.A., Kopell, N.J., 2005. Orthogonal arrangement of rhythm-generating microcircuits in the hippocampus. *Proc. Natl. Acad. Sci. U. S. A.* 102, 13295–13300.
- Golding, N.L., Staff, N.P., Spruston, N., 2002. Dendritic spikes as a mechanism for cooperative long-term potentiation. *Nature* 418, 326–331.
- Gratton, G., Coles, M.G., Donchin, E., 1983. A new method for off-line removal of ocular artifact. *Electroencephalogr. Clin. Neurophysiol.* 55, 468–484.
- Gray, C.M., Konig, P., Engel, A.K., Singer, W., 1989. Oscillatory responses in cat visual cortex exhibit inter-columnar synchronization which reflects global stimulus properties. *Nature* 338, 334–337.
- Isler, J.R., Grose-Fifer, J., Fifer, W.P., Housman, S., Stark, R.I., Grieve, P.G., 2007. Frequency domain analyses of neonatal flash VEP. *Pediatr. Res.* 62, 581–585.
- Jensen, O., Colgin, L.L., 2007. Cross-frequency coupling between neuronal oscillations. *Trends Cogn. Sci.* 11, 267–269.
- Kahana, M.J., Seelig, D., Madsen, J.R., 2001. Theta returns. *Curr. Opin. Neurobiol.* 11, 739–744.
- Lachaux, J.P., Rodriguez, E., Martinerie, J., Adam, C., Hasboun, D., Varela, F.J., 2000. A quantitative study of gamma-band activity in human intracranial recordings triggered by visual stimuli. *Eur. J. Neurosci.* 12, 2608–2622.
- Lakatos, P., Shah, A.S., Knuth, K.H., Ulbert, I., Karmos, G., Schroeder, C.E., 2005. An oscillatory hierarchy controlling neuronal excitability and stimulus processing in the auditory cortex. *J. Neurophysiol.* 94, 1904–1911.
- Luria, A.R., 1973. *The Working Brain*, Vol. Basic Books, New York.
- Nikias, C.L., Petropulu, A.P., 1993. *Higher-Order Spectra Analysis: a Nonlinear Signal Processing Framework*, Vol. PTR Prentice Hall, Englewood Cliffs, N.J.
- Nunez, P.L., 1981. *Electric Fields and the Brain*, Vol. Oxford University Press, New York.
- O'Keefe, J., Recce, M.L., 1993. Phase relationship between hippocampal place units and the EEG theta rhythm. *Hippocampus* 3, 317–330.
- Palva, J.M., Palva, S., Kaila, K., 2005. Phase synchrony among neuronal oscillations in the human cortex. *J. Neurosci.* 25, 3962–3972.
- Palva, S., Palva, J.M., 2007. New vistas for alpha-frequency band oscillations. *Trends Neurosci.* 30, 150–158.
- Perrin, F., Pernier, J., Bertrand, O., Giard, M.H., Echallier, J.F., 1987. Mapping of scalp potentials by surface spline interpolation. *Electroencephalogr. Clin. Neurophysiol.* 66, 75–81.
- Pfurtscheller, G., Flotzinger, D., Neuper, C., 1994. Differentiation between finger, toe and tongue movement in man based on 40 Hz EEG. *Electroencephalogr. Clin. Neurophysiol.* 90, 456–460.
- Pfurtscheller, G., Andrew, C., 1999. Event-related changes of band power and coherence: methodology and interpretation. *J. Clin. Neurophysiol.* 16, 512–519.
- Ranganath, C., Rainer, G., 2003. Neural mechanisms for detecting and remembering novel events. *Nat. Rev. Neurosci.* 4, 193–202.
- Rodriguez, E., George, N., Lachaux, J.P., Martinerie, J., Renault, B., Varela, F.J., 1999. Perception's shadow: long-distance synchronization of human brain activity. *Nature* 397, 430–433.
- Schack, B., Vath, N., Petsche, H., Geissler, H.G., Moller, E., 2002. Phase-coupling of theta-gamma EEG rhythms during short-term memory processing. *Int. J. Psychophysiol.* 44, 143–163.
- Sokolov, E.N., 1990. The orienting response, and future directions of its development. *Pavlovian J. Biol. Sci.* 25, 142–150.
- Srinivasan, R., Nunez, P.L., Silberstein, R.B., 1998. Spatial filtering and neocortical dynamics: estimates of EEG coherence. *IEEE Trans. Biomed. Eng.* 45, 814–826.
- Tallon-Baudry, C., Bertrand, O., Delpuech, C., Pernier, J., 1996. Stimulus specificity of phase-locked and non-phase-locked 40 Hz visual responses in human. *J. Neurosci.* 16, 4240–4249.
- Varela, F., Lachaux, J.P., Rodriguez, E., Martinerie, J., 2001. The brainweb: phase synchronization and large-scale integration. *Nat. Rev. Neurosci.* 2, 229–239.
- von Stein, A., Chiang, C., Konig, P., 2000. Top-down processing mediated by interareal synchronization. *Proc. Natl. Acad. Sci. U. S. A.* 97, 14748–14753.